



## Article

# AtZAT4, a C<sub>2</sub>H<sub>2</sub>-Type Zinc Finger Transcription Factor from *Arabidopsis thaliana*, Is Involved in Pollen and Seed Development

A. Carolina Puentes-Romero<sup>1,2</sup>, Sebastián A. González<sup>1</sup>, Enrique González-Villanueva<sup>1</sup>, Carlos R. Figueroa<sup>2,3</sup>   
and Simón Ruiz-Lara<sup>1,2,\*</sup> 

- <sup>1</sup> Laboratorio de Genómica Funcional, Institute of Biological Sciences, Universidad de Talca, Talca 3460000, Chile; apuentes@utalca.cl (A.C.P.-R.); sgonzalez@utalca.cl (S.A.G.); egonzale@utalca.cl (E.G.-V.)  
<sup>2</sup> Millennium Nucleus for the Development of Super Adaptable Plants (MN-SAP), Santiago 8340755, Chile; cfigueroa@utalca.cl  
<sup>3</sup> Laboratory of Plant Molecular Physiology, Institute of Biological Sciences, Universidad de Talca, Talca 3460000, Chile  
\* Correspondence: sruiz@utalca.cl

**Abstract:** Pollen plays an essential role in plant fertility by delivering the male gametes to the embryo sac before double fertilization. In several plant species, including *Arabidopsis*, C<sub>2</sub>H<sub>2</sub>-type zinc-finger transcription factors (TFs) have been involved in different stages of pollen development and maturation. ZINC FINGER of *Arabidopsis thaliana* 4 (AtZAT4) is homologous to such TFs and subcellular localization analysis has revealed that AtZAT4 is located in the nucleus. Moreover, analysis of *AtZAT4* expression revealed strong levels of it in flowers and siliques, suggesting a role of the encoded protein in the regulation of genes that are associated with reproductive development. We characterized a T-DNA insertional heterozygous mutant *Atzat4* (+/−). The relative gene expression analysis of *Atzat4* (+/−) showed significant transcript reductions in flowers and siliques. Furthermore, the *Atzat4* (+/−) phenotypic characterization revealed defects in the male germline, showing a reduction in pollen tube germination and elongation. *Atzat4* (+/−) presented reduced fertility, characterized by a smaller silique size compared to the wild type (WT), and a lower number of seeds per silique. Additionally, seeds displayed lower viability and germination. Altogether, our data suggest a role for AtZAT4 in fertilization and seed viability, through the regulation of gene expression associated with reproductive development.

**Keywords:** pollen development; seed development; zinc-finger proteins; ZAT; *Arabidopsis thaliana*



**Citation:** Puentes-Romero, A.C.; González, S.A.; González-Villanueva, E.; Figueroa, C.R.; Ruiz-Lara, S. AtZAT4, a C<sub>2</sub>H<sub>2</sub>-Type Zinc Finger Transcription Factor from *Arabidopsis thaliana*, Is Involved in Pollen and Seed Development. *Plants* **2022**, *11*, 1974. <https://doi.org/10.3390/plants11151974>

Academic Editor: Stefano Del Duca

Received: 10 June 2022

Accepted: 27 July 2022

Published: 29 July 2022

**Publisher's Note:** MDPI stays neutral with regard to jurisdictional claims in published maps and institutional affiliations.



**Copyright:** © 2022 by the authors. Licensee MDPI, Basel, Switzerland. This article is an open access article distributed under the terms and conditions of the Creative Commons Attribution (CC BY) license (<https://creativecommons.org/licenses/by/4.0/>).

## 1. Introduction

In angiosperm, the pollen grain is the male gametophyte. It plays a major role in plant fertility by generating sperm cells and conveying them to the embryo sac for double fertilization [1]. The correct pollen grain development, the functional pollen tube growth and sperm cells release are necessary for plant sexual reproduction and maintenance of genetic diversity [2]. Microgametophyte development involves the coordinated participation of sporophytic and gametophytic cell types, as well as the gene expressions that control their development in these tissues [3,4]. The *Arabidopsis* pollen grain development in the anther is well characterized. It occurs in the following three main stages: (i) microsporogenesis (microsporocytes meiosis), (ii) post-meiotic development of microspores (microspores release), and (iii) micro-gametogenesis (mitosis of microspores) [4]. These stages take place inside the anthers on the stamens. The stamen specification, like other floral whorls in *A. thaliana*, has been well characterized at the molecular level. According to the floral quartet model, genes encoding for transcription factors (TFs) of the MADS-box type participate in the identification of each flower whorl through quaternary protein complex formation. In this model, stamens are specified by class B+C+E genes [5–7].

Following the stamen specification, several TFs regulate specific gene expression within the anther, controlling the male germline development [8]. In this context, several C<sub>2</sub>H<sub>2</sub>-type Zinc-finger proteins (C<sub>2</sub>H<sub>2</sub>-ZFPs) participate in the regulatory network of anther and pollen grain development. To date, 176 genes that encode C<sub>2</sub>H<sub>2</sub>-ZFP have been identified in *Arabidopsis*, 189 in rice [9,10], 211 in maize [11], and 301 in *Brassica rapa* [12]. Most of the C<sub>2</sub>H<sub>2</sub>-ZFPs that are associated with plant growth, development and environmental stress responses are of Q-type, which present a conserved QALGGH motif in their zinc finger (ZF) domains. These have been exclusively identified in plants, suggesting one or more roles in processes unique to plants [13,14]. Accordingly, these TFs have been associated with specific plant abiotic stresses, including cold and salinity [15]. However, in addition to their role in stress response, several studies have shown their involvement during flower development. For example, SUPERMAN (SUP) is a Q-type C<sub>2</sub>H<sub>2</sub>-ZFP in *Arabidopsis*, with an ethylene-responsive element binding factor-associated amphiphilic repression (EAR) motif, which is essential for maintaining the boundary between stamens and carpels [16–18]. In addition, KNUCKLES (KNU) is a small protein containing a single C<sub>2</sub>H<sub>2</sub> ZF domain with an EAR-like active repression motif, which is essential during flower development for balancing cell proliferation and differentiation. Thus, KNU regulates cellular proliferation in the basal gynoecium tissues [13,19].

Genes encoding for C<sub>2</sub>H<sub>2</sub>-ZFPs, which have been described in *Petunia hybrida*, were temporarily and sequentially expressed during anther and pollen development [8]. Among them, TAPETUM DEVELOPMENT ZINC FINGER PROTEIN1 (TAZ1) plays an essential role in post-meiotic tapetum development [20], and MEIOSIS-ASSOCIATED ZINC FINGER PROTEIN 1 (MEZ1) participates in microsporocyte meiosis [21]. In *Arabidopsis*, two C<sub>2</sub>H<sub>2</sub>-ZFPs, DUO POLLEN 1 (DUO1)-ACTIVATED ZINC FINGER 1/2 (DAZ1/DAZ2) have been described in pollen development, specifically during germ cell division. Interestingly, these two TFs also display an EAR transcriptional repression motif [22]. Additionally, in *Arabidopsis*, the C<sub>2</sub>H<sub>2</sub>-ZFP MALE FERTILITY-ASSOCIATED ZINC FINGER PROTEIN 1 (MAZ1) is involved in pollen grain wall development [16]. In *Brassica campestris*, the C<sub>2</sub>H<sub>2</sub>-ZFP BcMF20 has been proposed to be involved in the development of tapetum [23]. Lastly, BrZFP38 from *B. rapa* is involved in the late development of pollen grain as well as pollination [24].

While a function of C<sub>2</sub>H<sub>2</sub> ZFPs has been assigned to pollen development, their involvement in embryo and seed development is less documented. TITAN-LIKE (TTL) is a protein with two atypical C<sub>2</sub>H<sub>2</sub> motifs. It plays a role in *Arabidopsis* endosperm development, particularly in endosperm nuclear divisions, and its defective activity leads to defects in the developing embryo [25]. *GmZFP1* from *Glycine max*, that encodes for a C<sub>2</sub>H<sub>2</sub> ZFP with a single ZF domain with a conserved QALGGH motif, has been associated with late stage seed development. *GmZFP1* was found to be strongly expressed from 45 days after flowering, while the gene expression was lower in the early seed development stage [26].

In this study, we characterized ZINC FINGER of *A. thaliana* 4 (AtZAT4; AT2G45120) as a C<sub>2</sub>H<sub>2</sub>-ZFP TF involved in reproductive development. AtZAT4 is an uncharacterized C<sub>2</sub>H<sub>2</sub>-ZFP but is associated with a similar function to AtZAT6 and AtZAT10, which are involved in biotic and/or abiotic stress responses [27,28]. The subcellular localization of AtZAT4 is in the nucleus and the transcriptional profile suggests that, in contrast to AtZAT6 and AtZAT10, AtZAT4 could be a regulating gene involved in pollen and seed development. We further characterized a heterozygous insertional mutant of *AtZAT4* [*Atzat4* (+/–)]. The mutant showed defects in the male germline, essentially during pollen germination and in the elongation tube. Accordingly, the fertility of *A. thaliana* was affected with the mutant exhibiting a lower number of developed seeds in comparison to the wild type (WT).

## 2. Results

### 2.1. AtZAT4 Is a Transcription Factor Similar to Other C<sub>2</sub>H<sub>2</sub>-ZFPs Associated with Reproductive Development in Model Plants

To know the evolutionary relationships of AtZAT4 with other C<sub>2</sub>H<sub>2</sub>-type zinc-finger proteins (C<sub>2</sub>H<sub>2</sub>-ZFP) involved in reproductive development, a multiple alignment (Figure S1) and a phylogenetic tree were constructed using the full-length amino acid sequences of AtZAT4 and other sequences of C<sub>2</sub>H<sub>2</sub>-ZFP from *Arabidopsis thaliana*, *Petunia hybrida*, *Silene latifolia*, *Brassica campestris* ssp. *chinensis* and *Brassica rapa* ssp. *chinensis*. The results showed that AtZAT4 belongs to the same clade as ZPT3-3 from *P. hybrida* [29], and ZPT3-1 from *S. latifolia* [30] (Figure 1). These results suggested that AtZAT4 is a C<sub>2</sub>H<sub>2</sub>-ZF transcription factor (TF) and is evolutionarily closest to TFs associated with reproductive development.

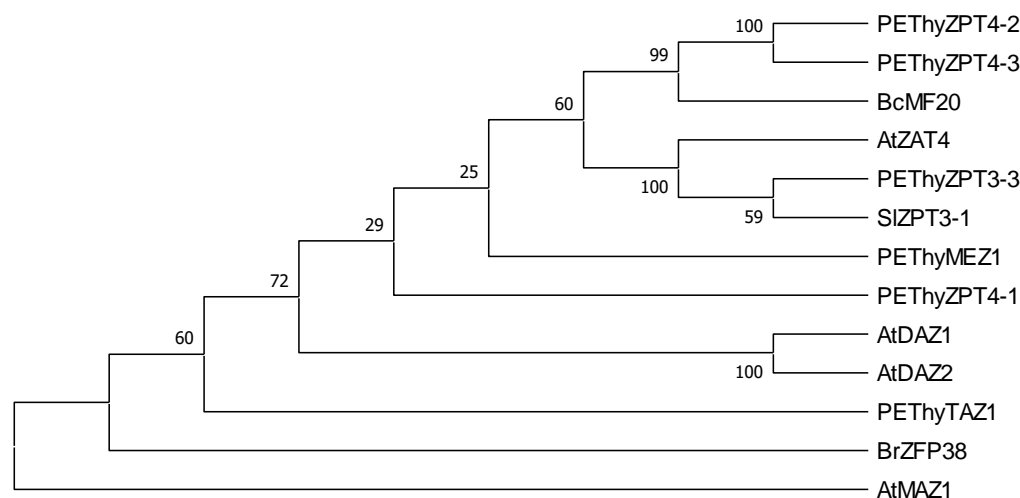


**Figure 1.** Molecular phylogenetic tree of AtZAT4 with other C<sub>2</sub>H<sub>2</sub>-Zinc Finger Proteins (C<sub>2</sub>H<sub>2</sub>-ZFPs). The tree was obtained from the multiple alignments of the deduced AtZAT4 and other C<sub>2</sub>H<sub>2</sub>-ZFPs following the Neighbor-Joining method in the MEGA-X package with 1000 replicates for bootstrap values. For details, see Section 4.

To determine the AtZAT4 subcellular localization, we transiently expressed a carboxyl-terminal fusion of AtZAT4 to the green fluorescent protein (GFP) under the control of CaMV 35S promoter in onion epidermal cells using the bombardment transformation method. The signal of AtZAT4:sGFP was observed only in the nucleus, while the control showed a GFP signal in both the nucleus and cytoplasm. It is important to note that GFP is a small protein that diffuses in a non-specific way through nuclear pores [31]. The subcellular localization of AtZAT4 was consistent not only with the nuclear localization signal (NLS) in silico prediction (Figure S1), but also with a function of AtZAT4 as a TF (Figure 2).

To identify the putative role of *AtZAT4* in *A. thaliana* development, we studied the organ-specific transcriptional profile of this gene. For this purpose, we proceeded to measure the level of transcripts using reverse transcription-quantitative real-time PCR (RT-qPCR) in 5- and 10-day-old seedlings and in different *A. thaliana* vegetative and reproductive tissues. *AtZAT4* showed high levels of transcripts in reproductive tissue, specifically in flowers and siliques. The RT-qPCR analysis also revealed moderate expression in stems; however, the transcript levels decreased in young seedlings and roots (Figure 3). These results were in agreement with the expression of *AtZAT4* (AT2G45120) visualized in silico in the eFP-browser (<http://bar.utoronto.ca/efp/cgi-bin/efpWeb.cgi>, accessed on 21 April 2015), in which *AtZAT4* showed high levels of expression in mature pollen and stamens, and also in seeds.

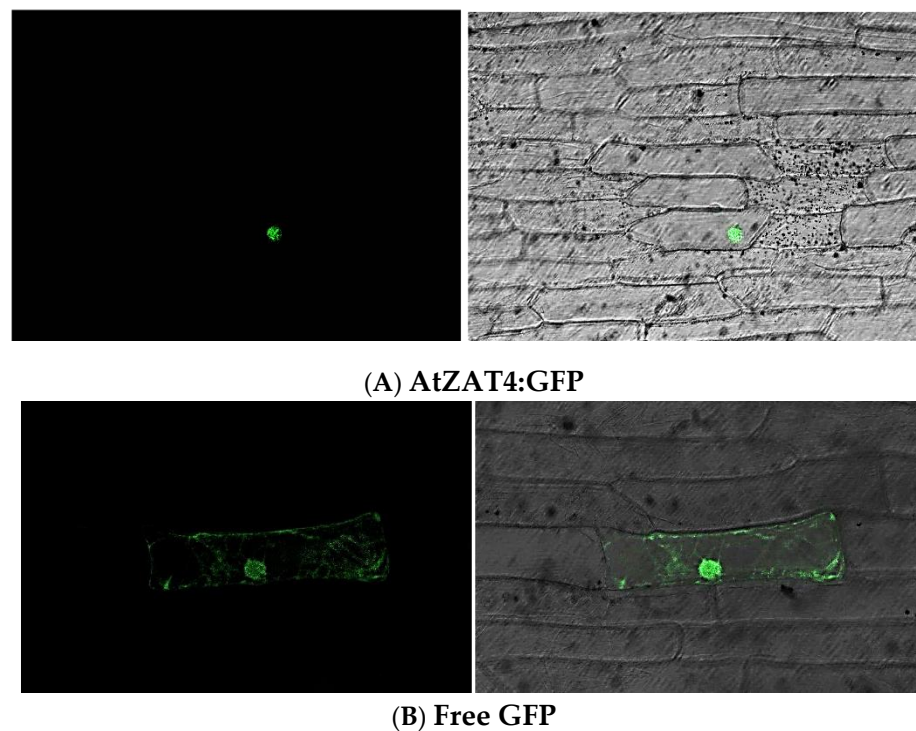


**Figure 2.** Subcellular localization of the AtZAT4 protein. (A) AtZAT4:GFP or (B) constructs carrying GFP were bombarded into onion epidermal cells. GFP and AtZAT4:GFP fusion proteins were under the control of the CaMV 35S promoter. After the bombardment, the samples were incubated for 24 h at 22 °C in the dark (left column) and then visualized by a confocal microscope (right column). Each experiment was done in triplicate resulting in the same fluorescence pattern. Bar = 100  $\mu$ m. For details, see Section 4.

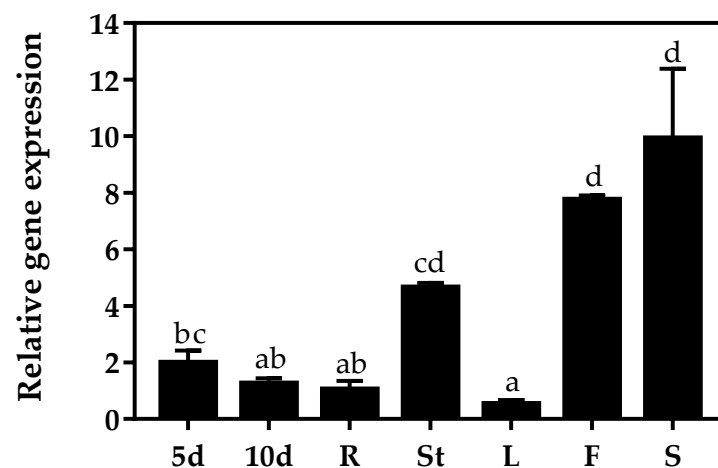


**Figure 3.** Gene expression profile of *AtZAT4* in vegetative and reproductive tissues of *Arabidopsis thaliana* and in 5- and 10-day-old seedlings. 5d seedlings of 5-day-old, 10d seedlings of 10-day-old, R root, St stem, L leaf, F flower, S silique. Values represent mean  $\pm$  SE ( $n = 3$ ). The constitutive expression of the gene *AtF-box* [32] and the  $2^{-\Delta\Delta Ct}$  method described by Livak and Schmittgen (2001) [33] were used for normalization. The transcript levels obtained for R were taken to assign the value one. Data correspond to the mean  $\pm$  SE. Significant differences ( $p \leq 0.05$ ) are shown with different letters. For details, see Section 4.

## 2.2. *AtZAT4* Is Essential for the Development of Reproductive Organs in *A. thaliana*

We used the line CS841944, which has a T-DNA insertion in the *AtZAT4* promoter region (Figure S2), to determine the *AtZAT4* function. The selection of seedlings in growth

medium revealed a survival rate of 48.9% instead of the 75% expected from Mendelian inheritance. Surviving seedlings were genotyped to determine the presence of the wild-type and/or the allele containing the T-DNA insertion (Figure S3). The total number of plants analyzed ( $n = 47$ ) showed the presence of both alleles simultaneously, indicating that they corresponded to heterozygotes [*Atzat4* (+/–)] (Figure S3B). The absence of homozygous seedlings for the allele containing the insertion suggested that this genotype was not viable. Therefore, these results might be an indicator that insertion in *AtZAT4* confers infertility or that it is lethal at an early embryonic stage.

To analyze the *AtZAT4* relative expression in *Atzat4* (+/–) and WT plants, an RT-qPCR of different vegetative and reproductive organs was performed. The results revealed that *AtZAT4* expression was significantly reduced in flowers and siliques in *Atzat4* (+/–), compared to the expression shown in WT plants (Figure 4). These reductions in the expression of *AtZAT4* observed in the *Atzat4* (+/–) plants suggested a possible role of this gene in the reproductive development of *A. thaliana*.

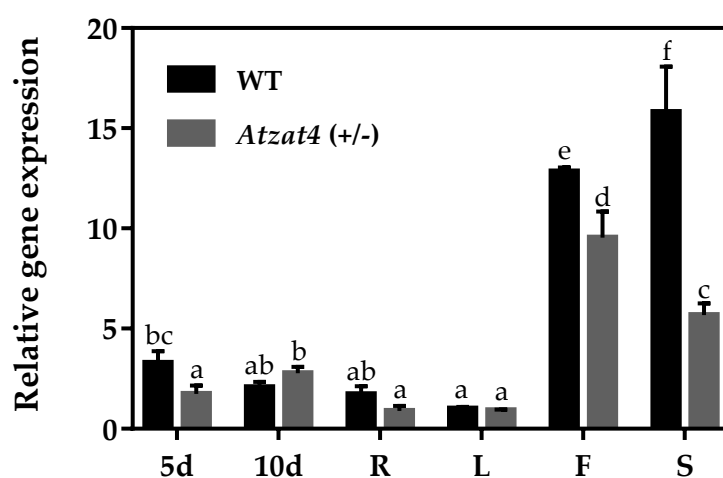


**Figure 4.** Gene expression profile of *Atzat4* (+/–) in vegetative and reproductive tissues of *Arabidopsis thaliana* and in 5- and 10-day-old seedlings. **5d** Five-day-old seedlings, **10d** Ten-day-old seedlings, **R** root, **L** leaf, **F** flower, **S** silique. Values represent mean  $\pm$  SE ( $n = 3$ ). The constitutive expression of the gene *AtF-box* [32] and the  $2^{-\Delta\Delta Ct}$  method described by Livak and Schmittgen (2001) [33] were used for normalization. The transcript levels obtained for R were taken to assign the value one. Data correspond to the mean  $\pm$  SE. Significant differences ( $p \leq 0.05$ ) are shown with different letters. For details, see Section 4.

### 2.3. *Atzat4* (+/–) Shows Defects in the Male Germline

To evaluate the function of *AtZAT4* in reproductive development, we performed a characterization of the heterozygous mutant *Atzat4* (+/–). We first analyzed the male germline phenotype. The pollen grain viability was determined by using modified Alexander staining [34]. In this method, viable pollen grains show a magenta red coloration of the cytoplasm while aborted pollen shows green cell walls [35,36]. We observed no significant difference in pollen viability between *Atzat4* (+/–) and WT, both showing viability around 100% ( $n =$  pollen grains from 18 anthers of different flowers of each genotype) (Figure 5A,B). However, pollen tube germination and elongation in vitro revealed significant differences in the mutant *Atzat4* (+/–), compared to WT. In fact, *Atzat4* (+/–) showed reduced germination and smaller tubes in our conditions (Figure 5C–E). *Atzat4* (+/–) presented a 34% ( $102 \pm 3$ ) germination, compared to a 56% ( $168 \pm 4$ ) in WT (Figure 5C). In addition, *Atzat4* (+/–) pollen tubes presented reduced elongation, with  $164 \pm 6 \mu\text{m}$  compared to  $303 \pm 8 \mu\text{m}$  in WT (Figure 5D,E). These results indicated that *AtZAT4* activity was necessary for pollen grain germination and pollen tube elongation.

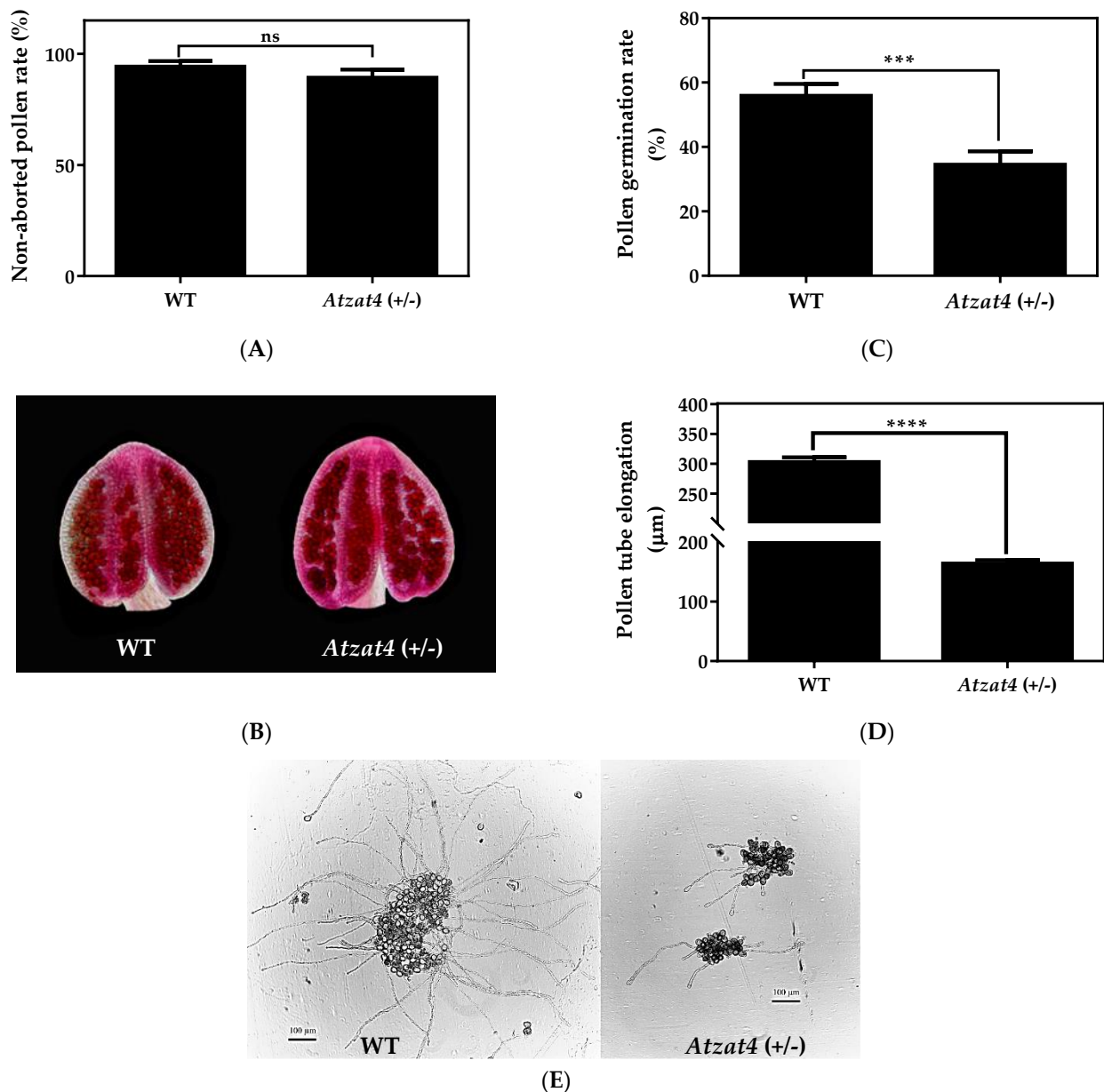


**Figure 5.** Male germline in *Atzat4 (+/-)* compared to WT in *Arabidopsis thaliana*. (A,B) Modified Alexander stain [34]. (B) Alexander red staining of pollen grains by anther, non-aborted pollen grains are stained red. (C–E) In vitro pollen grain germination and pollen tube elongation. (C) Quantification of germinated pollen grains ( $n = 300$  pollen grains analyzed). (D) Pollen tube elongation quantification ( $n = 300$  pollen grains germinated). (E) In vitro pollen grain germination and pollen tube elongation under the light microscope. In (A,C,D) data correspond to the mean  $\pm$  SE; \*\*\*\*  $p < 0.0001$ , \*\*\*  $p < 0.001$ , ns: not significant. In (B,E), bars = 100  $\mu\text{m}$ . For details, see Section 4.

#### 2.4. *Atzat4 (+/-)* Shows Defects in the Fertility

We further measured *Atzat4 (+/-)* fertility in comparison to WT. For this purpose, we decolored siliques and quantified the number of seeds. The results revealed a reduced number of seeds in *Atzat4 (+/-)*, which was associated with a greater number of unfertilized eggs (Figure 6A,B). Thus, we counted  $39 \pm 2$  seeds per silique on average in WT, while only  $27 \pm 1$  seeds per silique in *Atzat4 (+/-)*. We also quantified the siliques' sizes. The siliques of mutants were  $12 \pm 2$  mm in *Atzat4 (+/-)*, being shorter than WT, which accounted for  $14.5 \pm 1$  mm (Figure 6C). Then, viability and germination capacity assays of seeds were

performed. To determine seed viability, the Tetrazolium test was used according to Verma and Majee (2013) [37]. The results showed that the viability of seeds was significantly reduced in the mutant *Atzat4* (+/−) with a total of 60% ( $60 \pm 2$ ) compared to 98% ( $98 \pm 0.04$ ) in WT (Figure 6D,E). These differences seem to be explained by the high number of aborted seeds in the mutant phenotype (Figure 5B). The seed germination was also significantly reduced in *Atzat4* (+/−) with a 49% ( $49 \pm 2$ ) versus 88% ( $88 \pm 4$ ) in WT (Figure 6F). Taken together, these results indicated reduced fertility of *Atzat4* (+/−), suggesting that AtZAT4 was also involved in the development of the seed. Since the expression level of AtZAT4 in the *Atzat4* (+/−) mutants was insufficient for the correct development of seeds, a high number of ovules were aborted.

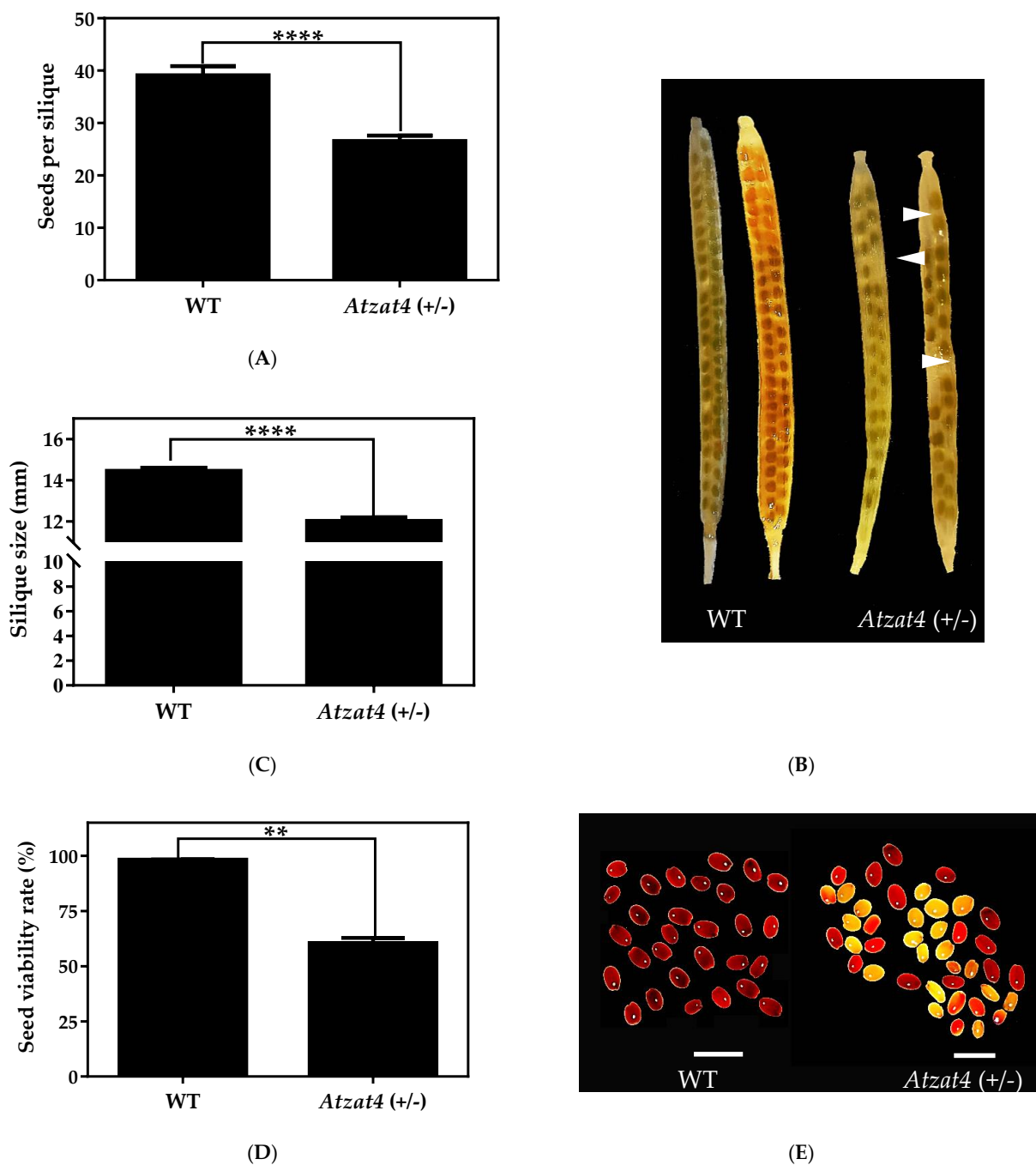
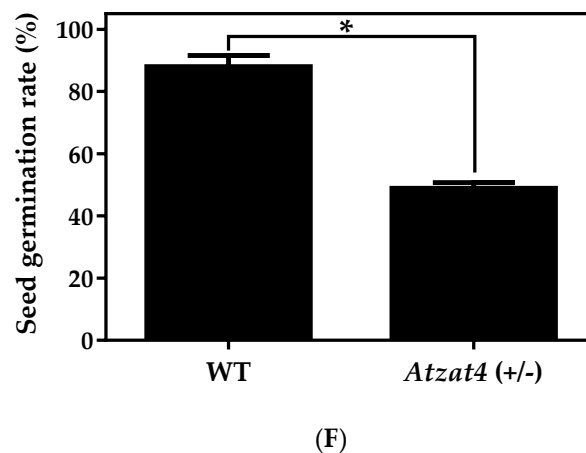


Figure 6. Cont.



**Figure 6.** Fertility in *Atzat4 (+/-)* compared to WT in *Arabidopsis thaliana*. (A) Seeds per silique quantification ( $n = 10$  siliques in triplicate). (B) Discolored siliques with developed seeds and unfertilized ovules (white arrowheads). (C) Silique size quantification ( $n = 10$  siliques in triplicate). (D) Viable seeds quantification using Tetrazolium test ( $n = 100$  seeds in triplicate). (E) Tetrazolium test, red staining shows viable seeds, unstained unviable seeds and pink stain indicates dead tissue. (F) Quantification of germinated seeds ( $n = 100$  seeds in triplicate). In (A,C,D,F) data correspond to the mean  $\pm$  SE; \*\*\*\*  $p < 0.0001$ , \*\*  $p < 0.01$ , \*  $p < 0.05$ . In (B,E), bars = 1 mm. For details, see Section 4.

### 3. Discussion

Several C<sub>2</sub>H<sub>2</sub>-type ZFPs have been described to participate in anther and pollen development in *Arabidopsis* and other model plant species [16,20–24]. *AtZAT4* was primarily identified by Mittler et al. (2006) [27] by evaluating the expression of some genes of the *AtZAT* family under different stress conditions, but so far *AtZAT4* from *A. thaliana* has not been characterized in male reproductive and seeds development.

The phylogenetic analysis revealed that *AtZAT4* is highly conserved with other C<sub>2</sub>H<sub>2</sub>-ZFPs described in the reproductive development of other plant species (Figures 1 and S1) [29,30]. *PETHyZPT3-3* and *SIZPT3-1* have three C<sub>2</sub>H<sub>2</sub>-ZF domains, the same as *AtZAT4*. The function of *PETHyZPT3-3* has been associated with reproductive development, where *PETHyZPT3-3* is expressed in stigma, style, ovary, and receptacle of petunia. Interestingly, *PETHyZPT3-3* activity could be related to pollen tube guidance [29]. Moreover, *SIZPT3-1* from *Silene latifolia* is expressed predominantly in male flowers and, to a lesser extent, in female ones [30]. These antecedents allow us to suggest that *AtZAT4* could be involved in the reproductive development of *Arabidopsis*.

*AtZAT4* is a C<sub>2</sub>H<sub>2</sub>-type ZFPs with three different types of the conserved plant-specific sequences QALGGH in all ZF domains: the first one is a K2-1 type, the second is a Q2-2 type, and the last one is Q2-3 type (Figure S1). Therefore, it has two invariant Q-type motifs [9]. Additionally, *AtZAT4* has an EAR repression motif, which has been associated with repressive activity and is found at the C-terminus of the proteins (Figure S1) [38]. Several studies have shown that C<sub>2</sub>H<sub>2</sub>-ZFPs containing QALGGH and EAR transcriptional repression motifs participate in the development of plant reproductive organs [16,19,22,24]. In addition, according to in silico prediction, *AtZAT4* has an NLS (Figure S1). This signal was functional, since the analysis of the subcellular localization showed that *AtZAT4* was localized in the nucleus (Figure 2). This suggests that *AtZAT4* could act as a transcriptional factor modulating the gene expression related to the reproductive development of *A. thaliana* in a similar way to other previously described C<sub>2</sub>H<sub>2</sub> ZFPs.

Members of the ZAT protein family have been associated with abiotic stress responses. For instance, *AtZAT12* has been involved in response to cold and oxidative stresses [39,40] while *AtZAT10* has been associated with plant responses to drought, salinity and cold stresses [27,41]. Furthermore, *AtZAT7* participates in tolerance to salt stress [42]. The *AtZAT4* transcriptional profile indicates a higher expression in flowers and siliques



(Figure 3), suggesting a role in reproductive organ development. As far as we know, no data is available about the role of the ZAT family in reproductive development. Although our results suggest that AtZAT4 might be involved in male and seed development, its involvement in stress response cannot be ruled out.

An insertional heterozygous T-DNA mutant was used to investigate the function of AtZAT4. Interestingly, *in vitro* seedling selection revealed that homozygous plants were not viable as all seedlings surviving DL-phosphinothricin herbicide were heterozygous [*Atzat4* (+/−)] (data not shown). This suggested that AtZAT4 was essential for the development of *A. thaliana*. In addition, transcriptional analysis by RT-qPCR revealed the *Atzat4* (+/−) mutant showed a significant reduction in AtZAT4 expression of flowers and siliques compared to WT (Figure 4). According to eFP-browser 2.0 (<http://bar.utoronto.ca/efp/cgi-bin/efpWeb.cgi> accessed on 19 November 2020), early stages in embryo and seed development showed high AtZAT4 expression. This could be related to the lack of viability of embryos homozygous in the insertional mutant, and, therefore, all germinated seedlings showed a WT allele.

The phenotype characterization of the *Atzat4* (+/−) mutant showed similar traits to other male-sterile plants [16,20,23,24]. We observed significant reduced germination and pollen tube elongation in the heterozygous insertional mutant compared with the WT (Figure 5C–E). Both characteristics are essential for the delivery of sperm cells into the ovary, and, thus, for double fertilization [43]. Poor germination and pollen tube elongation may indicate defects during anther and pollen development, as well as during pollen maturation [44]. This suggested that this TF plays an important role during anther and pollen development, and its defect causes male sterility, as other C<sub>2</sub>H<sub>2</sub>-type ZFPs, such as TAZ1 or BcMF20, involved in petunia and *B. campestris* tapetum development, respectively, or in pollen grain wall development as Arabidopsis MAZ1. It has been described that the loss of function of these C<sub>2</sub>H<sub>2</sub> ZFPs leads to a reduced germination capacity [16,20,23]. On the other hand, Lyu et al. (2020) [24] characterized several C<sub>2</sub>H<sub>2</sub> ZFPs in *B. rapa* ssp. *chinensis*. One of them is BrZFP38 with two EAR motifs and is functional during male germline development. Interestingly, BrZFP38 showed high expression in mature pollen grains, but also in the pollen tube during the germination and fertilization processes.

After a double fertilization process, the seed is formed from the ovule, and the fruit is differentiated from the carpel [45,46]. We characterized AtZAT4 in *A. thaliana* fertility. The results evidenced reduced fertility, with a lower number of seeds per silique and smaller silique size, as well as lower seed viability in comparison to WT (Figure 6). Similar to other C<sub>2</sub>H<sub>2</sub> ZFPs involved in pollen development, these results suggested a role for this TF in *A. thaliana* embryo and seed development. Defects in *DAZ1/DAZ2* from *A. thaliana*, which have two EAR motifs, result in abnormal pollen mitosis, and reduced fertility with a lack of embryo and seed development [22]. On the other hand, in petunia, MEZ1 showed incomplete embryo development in addition to defects during the male meiosis [21]. In our research, the TZ test revealed an approximation of the AtZAT4 role in embryo development showing a high number of aborted seeds in the mutant, and, thus, an abnormal embryo development. This could suggest that AtZAT4 is involved in embryo development like other C<sub>2</sub>H<sub>2</sub>-ZFPs. In summary, the high AtZAT4 expression level in siliques, in addition to the reduced number of seeds per silique, and the lower seed viability and germination rate observed in *Atzat4* (+/−) suggest a putative role during AtZAT4 embryo and seed development. Nevertheless, more studies are needed to confirm this hypothesis.

## 4. Materials and Methods

### 4.1. Plant Material and Growth Conditions

*Arabidopsis thaliana* wild type (WT) plants [ecotype Columbia-0 (Col-0)] and mutants with insertion of T-DNA in the promoter region of *AtZAT4* (CS841944) were obtained from *Arabidopsis Biological Resource Center* (ABRC, <https://abrc.osu.edu> accessed on 9 July 2015). The plants were grown on a sterile substrate composed of perlite, vermiculite, and peat (1:1:1), and maintained in greenhouse conditions with long daytime photoperiod (16 h

light/8 h dark). Plants were fertilized every two weeks with commercial Ultrasol<sup>®</sup> solution (SQM, Santiago, Chile), and kept until obtaining reproductive structures (flower buds, flowers and siliques) for phenotyping assays, as well as for DNA or RNA extraction.

#### 4.2. Genotyping and Plant Selection

Seeds from *A. thaliana* self-pollinated heterozygous plants *Atzat4* (+/−) ( $n = 96$ ) were germinated on MS (Murashige and Skoog) culture medium with Gamborg vitamins (PhytoTech Labs, Lenexa, KS, USA), supplemented with 100 mg/L of DL-phosphinothricin herbicide (or glufosinate ammonium; PhytoTech Labs, Lenexa, KS, USA), to eliminate WT plants generated during self-pollination and to select those which contained the T-DNA insertion. The surviving plants were analyzed by PCR on gDNA to determine the presence of both the wild-type allele and the T-DNA insertion-containing allele (pCSA110; Table S1). Seedlings with true leaves (18 day-old) were transplanted into pots containing a mixture of perlite:vermiculite:peat (1:1:1). *Arabidopsis Atzat4* (+/−) plants were selected by application of 120 mg/L of BASTA<sup>®</sup> 14 SL herbicide (glufosinate ammonium; Bayer, Frankfurt, Germany) and Silwet<sup>®</sup> L-77 (polyalkyleneoxide modified heptamethyltrisiloxane; Momentive Inc., Waterford, NY, USA). Three applications were made every two days by spraying, along with an application of herbicide to WT plants as a control. The presence of T-DNA in mutant plants was analyzed by PCR on gDNA using specific primers for the insertion (Table S1).

#### 4.3. RNA Isolation and cDNA Synthesis

For RNA extraction, the samples were immediately frozen in liquid nitrogen and stored at  $-80$  °C. Total RNA was extracted from different tissues of *A. thaliana* and also from 5- and 10-day-old seedlings, using the SV Total RNA Isolation System kit (Promega, Madison, WI, USA). From this, RNA integrity was visualized by 2% ( $w/v$ ) agarose gel electrophoresis, and RNA concentration and purity ( $OD_{260}/OD_{280}$  ratio  $> 1.95$ ) were determined with an Infinite<sup>®</sup> 200 PRO NanoQuant (Tecan, Männedorf, Switzerland). All RNA samples were treated with Turbo<sup>™</sup> DNase (Invitrogen, Waltham, MA, USA) to remove contaminant DNA traces. To prepare first-strand cDNA, 2 µg of total RNA were reverse transcribed in a 20 µL reaction using the oligo d(T) and AffinityScript qPCR cDNA Synthesis Kit (Agilent Technologies, Inc., Santa Clara, CA, USA), following manufacturer's instructions.

#### 4.4. Subcellular Localization of the AtZAT4-GFP Fusion Protein

First, in silico prediction of a Nuclear Localization Signal (NLS) was performed by NLStradamus online software (<http://www.moseslab.csb.utoronto.ca/NLStradamus/> accessed on 21 April 2015) [47]. Subsequently, the cDNA of *AtZAT4* was cloned in pGEM<sup>®</sup>-T Vector Easy (Promega, Madison, WI, USA) without stop-codon and with a cleavage site for *NcoI* at its 3' end. The resulting plasmid was treated with *NcoI* enzyme and the released fragment was ligated into the pGFPau vector, containing GFP, under the control of the Cauliflower Mosaic Virus (CaMV) 35S promoter. The constructs were transferred into onion epidermal cells by particle bombardment using a Bio-Rad Biolistic PDS 1000/He system. The samples were incubated for 24 h at 22 °C in darkness. The protein localization was determined by a Leica SP2 confocal microscope (Leica, Wetzlar, Germany).

#### 4.5. Analysis of Gene Expression

The relative *AtZAT4* expression was analyzed by reverse transcription-quantitative real-time PCR (RT-qPCR) in different tissues of *A. thaliana* and in 5- and 10-day-old seedlings of WT and *Atzat4* (+/−) using a Stratagene Mx3000P QPCR System (Agilent Technologies, Inc., Santa Clara, CA, USA). The 2X Maxima<sup>®</sup> SYBR Green/ROX qPCR Master Mix (Thermo Scientific, Waltham, MA, USA) was used in all reactions, according to the protocol described by the manufacturer. For each of the three biological replicates used, RT-qPCR was carried out in triplicate, using 10 µL of Master Mix, 0.5 µL of 250 nM primers, 2 µL of cDNA (25 ng/ µL), and nuclease-free water to a final volume of 20 µL. Amplification was followed

by a melting curve analysis with continuous fluorescence acquisition during the 55–95 °C melt. The gene expression was normalized against *AtF-box* (AT5G15710) [32], and the fold change of gene transcript levels was calculated using the  $2^{-\Delta\Delta C_t}$  method [33].

#### 4.6. Construction and Analysis of Phylogenetic Tree

C<sub>2</sub>H<sub>2</sub> ZFP sequences were obtained from the NCBI database (<https://www.ncbi.nlm.nih.gov/> accessed on 6 April 2015). Multiple protein sequence alignments were done by using the MEGA X software (version 11.0) [48] with ClustalW, and default parameters [49]. For the alignment edition, we used BioEdit (version 7.2) [50]. The identification of the C<sub>2</sub>H<sub>2</sub> Zinc finger domains was performed in InterProScan (<https://www.ebi.ac.uk/interpro/search/sequence/> accessed on 21 April 2015) [51]. The nuclear localization signal was determined in NLStradamus (<http://www.moseslab.csb.utoronto.ca/NLStradamus/> accessed on 21 April 2015) [47], and the EAR motif was determined literature-based [52]. On the other hand, phylogenetic analysis was performed with MEGA X software (version 11.0 Philadelphia, USA) [48] by the Neighbor-Joining method [53], and the bootstrap resampling method using 1000 replicates [54]. The GenBank accession numbers of plant ZFPs used for phylogenetic tree are the following: *Arabidopsis thaliana* AtZAT4 (AT2G45120), AtMAZ1 (AT5G15480), AtDAZ1 (AT2G17180), AtDAZ2 (AT4G35280); *Petunia hybrida* PETHyZPT3-3 (BAA96071), PETHyZPT4-2 (BAA19926), PETHyZPT4-3 (BAA20137), PETHyTAZ1 (BAA19113), PETHyZPT4-1 (BAA19114), PETHyMEZ1 (BAA19110); *Silene latifolia* SIZPT3-1 (AAY40249); *Brassica campestris* ssp. *chinensis* (ADK92391). The sequence of BrZFP38 from *Brassica rapa* ssp. *chinensis* (Bra011631) was obtained from BRAD (<http://brassicadb.cn/> accessed on 5 January 2021).

#### 4.7. Pollen Viability

For the pollen grain viability analysis, modified Alexander staining was performed [34]. *Arabidopsis* WT and mutant *Atzat4* (+/−) flowers in stage 12 of flower development [55,56] from three different plants were dissected under the Olympus SZ30 magnifier (Tokyo, Japan) to obtain complete stamens. They were fixed and discolored in Carnoy solution, with absolute ethanol, chloroform, and acetic acid (6:3:1) for at least 2 h. The fixed stamens were placed on a slide with 2–4 drops of modified Alexander solution, following the described protocol [34]. Subsequently, the staining was visualized under the optical microscope (Wild Leitz GMBH, Germany). Later, the number of viable pollen grains from the anthers of three biological replicas was quantified, thus obtaining the rate of viability for each genotype.

#### 4.8. In Vitro Pollen Tube Germination and Elongation

For the pollen tube germination and elongation analysis, four dehiscent anthers (anthesis) of *Arabidopsis* from WT and *Atzat4* (+/−) from three different plants were used. The pollen grains of each flower were deposited on slides with a solid germination medium with 200 µL of 500 mM KCl, 200 µL of 500 mM CaCl<sub>2</sub>, 200 µL of 100 mM MgSO<sub>4</sub>, 200 µL of 1% (w/v) H<sub>3</sub>BO<sub>3</sub>, 4 g sucrose and 0.3 g agarose [1.5% (w/v)] for 20 mL of the final solution, pH 7.5. The samples were covered with a dialysis membrane and were kept in a humid chamber for 6 h at 28 °C. The pollen germination and elongation were visualized under a 10X lens in the Zeiss LSM700 microscope in brightfield and the image analysis was performed using ZEN-Zeiss software (Oberkochen, Germany). Finally, the germinated pollen grains quantification and the length of the pollen tubes measurement were performed in ImageJ software (National Institute of Health, Bethesda, Maryland, USA). Using these results, the pollen grain germination percentage and pollen tube size average were calculated.

#### 4.9. Seeds per Siliques and Silique Size Quantification

Discoloration of mature, non-dehiscent silique was performed for WT and *Atzat4* (+/−); The seeds quantification was performed under the Olympus SZ30 magnifying glass (Tokyo,

Japan). Seeds of 10 siliques from three different plants were quantified. Furthermore, the sizes of 12 mature non-dehiscent siliques from three different plants were quantified for the two genotypes.

#### 4.10. Seed Viability and Germination

Seed viability analysis was performed using the tetrazolium test (2,3,5-triphenyl tetrazolium chloride; TZ) for WT and *Atzat4* (+/−) plants. TZ precipitates to 2,3,5-triphenyl formazan red by the activity of dehydrogenases present in living cells [37,57,58]. One hundred seeds were taken in three technical replicates, with the protocol described by Verma & Majee (2013) [37]. Finally, the quantification of viable, non-viable and defective seeds was carried out under the Olympus SZ30 magnifying glass (Tokyo, Japan). At the same time, a germination analysis of Arabidopsis seeds for two genotypes was performed in an MS culture medium with Gamborg vitamins (PhytoTech Labs, Lenexa, KS, USA) and 3% (*w/v*) sucrose. We used ~50 seeds in triplicate, which were disinfected. Subsequently, the seeds were placed in a growth chamber, and the germinated seeds were quantified on the third day of growth.

#### 4.11. Statistical Analysis

Statistical analyses were performed by using the software R and Rcmdr package ([http://knuth.uca.es/R/doku.php?id=instalacion\\_de\\_r\\_y\\_rcmdr:r-uca](http://knuth.uca.es/R/doku.php?id=instalacion_de_r_y_rcmdr:r-uca) accessed on 10 January 2018) (John Fox, Hamilton, ON, Canada). The analyses included T-Student for phenotypic characterization and one-way ANOVA for relative expression data using Tukey test at  $p \leq 0.05$  to determine significant differences between means. The results were expressed as means  $\pm$  standard error (SE).

## 5. Conclusions

In conclusion, we have characterized AtZAT4, for the first time, at the functional level in the *A. thaliana* reproductive development. The *Atzat4* (+/−) insertional mutant revealed a reduced expression in flowers and siliques, and the phenotypic characterization suggested a reduced activity of this transcription factor, which resulted in defects in male germline and fertility of *A. thaliana*. *Atzat4* (+/−) presented reduced germination and pollen tube elongation, as well as a lower number of seeds per silique and a reduced fruit size. In addition, *Atzat4* (+/−) revealed lower viability and seed germination. Based on these antecedents, we suggest that AtZAT4 regulates the expression of genes involved in pollen development, and is likely to also regulate genes implicated in embryo and seed development.

**Supplementary Materials:** The following supporting information can be downloaded at: <https://www.mdpi.com/article/10.3390/plants11151974/s1>, Figure S1: Multiple sequence alignment of deduced amino acid sequences of AtZAT4 and others C2H2 zinc-finger proteins (C2H2-ZFPs); Figure S2: Proportional schematic representation of T-DNA insertion into the Arabidopsis thaliana genome and inside the AtZAT4 promoter region; Figure S3: *Atzat4* (+/−) mutant genotyping from Arabidopsis thaliana; Table S1: Nucleotide sequence of primers used in RT-qPCR and in genotyping analyses.

**Author Contributions:** A.C.P.-R., S.A.G., E.G.-V. and S.R.-L. conceived the project and designed the experiments; A.C.P.-R. and S.A.G. performed the experiments; A.C.P.-R., E.G.-V., C.R.F. and S.R.-L. analyzed the experiment data and wrote the manuscript. All authors have read and agreed to the published version of the manuscript.

**Funding:** This research was funded by the National Research and Development Agency (ANID, Chile) grants FONDECYT/Regular 1161237 to E.G.-V., and Millennium Science Initiative Program-NCN2021\_010 to A.C.P.-R., C.R.F. and S.R.-L., A.C.P.-R. and S.A.G. were supported by ANID through ‘Beca Doctorado Nacional’ Nos. 21140896 and 21060500, respectively.

**Data Availability Statement:** Not applicable.

**Acknowledgments:** We thank Erwan Michard (Institute of Biological Sciences, Universidad de Talca) for his critical reading of the manuscript.

**Conflicts of Interest:** The authors declare no conflict of interest.

## References

1. Borg, M.; Brownfield, L.; Twell, D. Male gametophyte development: A molecular perspective. *J. Exp. Bot.* **2009**, *60*, 1465–1478. [[CrossRef](#)]
2. Wilson, Z.A.; Zhang, D.-B. From *Arabidopsis* to rice: Pathways in pollen development. *J. Exp. Bot.* **2009**, *60*, 1479–1492. [[CrossRef](#)] [[PubMed](#)]
3. Wang, J.; Qiu, X.; Li, Y.; Deng, Y.; Shi, T. A transcriptional dynamic network during *Arabidopsis thaliana* pollen development. *BMC Syst. Biol.* **2011**, *5*, S8. [[CrossRef](#)] [[PubMed](#)]
4. Gómez, J.F.; Talle, B.; Wilson, Z.A. Anther and pollen development: A conserved developmental pathway. *J. Integr. Plant Biol.* **2015**, *57*, 876–891. [[CrossRef](#)]
5. Theißen, G. Development of floral organ identity: Stories from the MADS house. *Curr. Opin. Plant Biol.* **2001**, *4*, 75–85. [[CrossRef](#)]
6. Becker, A.; Theißen, G. The major clades of MADS-box genes and their role in the development and evolution of flowering plants. *Mol. Phylogenet. Evol.* **2003**, *29*, 464–489. [[CrossRef](#)]
7. Theißen, G.; Melzer, R.; Ruümpler, F. MADS-domain transcription factors and the floral quartet model of flower development: Linking plant development and evolution. *Development* **2016**, *143*, 3259–3271. [[CrossRef](#)] [[PubMed](#)]
8. Kobayashi, A.; Sakamoto, A.; Kubo, K.; Rybka, Z.; Kanno, Y.; Takatsuji, H. Seven zinc-finger transcription factors are expressed sequentially during the development of anthers in petunia. *Plant J.* **1998**, *13*, 571–576. [[CrossRef](#)] [[PubMed](#)]
9. Englbrecht, C.C.; Schoof, H.; Böhm, S. Conservation, diversification and expansion of C<sub>2</sub>H<sub>2</sub> zinc finger proteins in the *Arabidopsis thaliana* genome. *BMC Genom.* **2004**, *5*, 39. [[CrossRef](#)] [[PubMed](#)]
10. Agarwal, P.; Arora, R.; Ray, S.; Singh, A.K.; Singh, V.P.; Takatsuji, H.; Kapoor, S.; Tyagi, A.K. Genome-wide identification of C<sub>2</sub>H<sub>2</sub> zinc-finger gene family in rice and their phylogeny and expression analysis. *Plant Mol. Biol.* **2007**, *65*, 467–485. [[CrossRef](#)]
11. Wei, K.; Pan, S.; Li, Y. Functional Characterization of Maize C<sub>2</sub>H<sub>2</sub> Zinc-Finger Gene Family. *Plant Mol. Biol. Rep.* **2016**, 761–776. [[CrossRef](#)]
12. Alam, I.; Batool, K.; Cui, D.L.; Yang, Y.Q.; Lu, Y.H. Comprehensive genomic survey, characterization and expression analysis of C<sub>2</sub>H<sub>2</sub> zinc finger protein gene family in *Brassica rapa* L. *PLoS ONE* **2019**, *10*, e0216071. [[CrossRef](#)]
13. Lyu, T.; Cao, J. Cys2/His2 zinc-finger proteins in transcriptional regulation of flower development. *Int. J. Mol. Sci.* **2018**, *19*, 2589. [[CrossRef](#)] [[PubMed](#)]
14. Takatsuji, H. Zinc-finger transcription factors in plants. *Cell. Mol. Life Sci.* **1998**, *54*, 582–596. [[CrossRef](#)] [[PubMed](#)]
15. Wang, K.; Ding, Y.; Cai, C.; Chen, Z.; Zhu, C. The role of C<sub>2</sub>H<sub>2</sub> zinc finger proteins in plant responses to abiotic stresses. *Physiol. Plant.* **2019**, *165*, 690–700. [[CrossRef](#)] [[PubMed](#)]
16. Lyu, T.; Hu, Z.; Liu, W.; Cao, J. *Arabidopsis* Cys2/His2 zinc-finger protein MAZ1 is essential for intine formation and exine pattern. *Biochem. Biophys. Res. Commun.* **2019**, *518*, 299–305. [[CrossRef](#)] [[PubMed](#)]
17. Dathan, N.; Zaccaro, L.; Esposito, S.; Isernia, C.; Omichinski, J.G.; Riccio, A.; Pedone, C.; Di Blasio, B.; Fattorusso, R.; Pedone, P.V.; et al. The *Arabidopsis* SUPERMAN protein is able to specifically bind DNA through its single Cys2-His2 zinc finger motif. *Nucleic Acids Res.* **2002**, *30*, 4945–4951. [[CrossRef](#)]
18. Sakai, H.; Medrano, L.J.; Meyerowitz, E. Role of *SUPERMAN* in maintaining *Arabidopsis* floral whorl boundaries. *Nature* **1995**, *378*, 199–203. [[CrossRef](#)]
19. Payne, T.; Johnson, S.D.; Koltunow, A.M. *KNUCKLES (KNU)* encodes a C<sub>2</sub>H<sub>2</sub> zinc-finger protein that regulates development of basal pattern elements of the *Arabidopsis* gynoecium. *Development* **2004**, *131*, 3737–3749. [[CrossRef](#)] [[PubMed](#)]
20. Kapoor, S.; Kobayashi, A.; Takatsuji, H. Silencing of the tapetum-specific zinc finger gene *TAZ1* causes premature degeneration of tapetum and pollen abortion in petunia. *Plant Cell* **2002**, *14*, 2353–2367. [[CrossRef](#)]
21. Kapoor, S.; Takatsuji, H. Silencing of an anther-specific zinc-finger gene, *MEZ1*, causes aberrant meiosis and pollen abortion in petunia. *Plant Mol. Biol.* **2006**, *61*, 415–430. [[CrossRef](#)]
22. Borg, M.; Rutley, N.; Kagale, S.; Hamamura, Y.; Gherghinoiu, M.; Kumar, S.; Sari, U.; Esparza-Franco, M.A.; Sakamoto, W.; Rozwadowski, K.; et al. An EAR-Dependent Regulatory Module Promotes Male Germ Cell Division and Sperm Fertility in *Arabidopsis*. *Plant Cell* **2014**, *26*, 2098–2113. [[CrossRef](#)]
23. Han, Y.Y.; Zhou, H.-Y.; Xu, L.-A.; Liu, X.-Y.; Fan, S.-X.; Cao, J.-S. The zinc-finger transcription factor *bcmf20* and its orthologs in Cruciferae which are required for pollen development. *Biochem. Biophys. Res. Commun.* **2018**, *503*, 998–1003. [[CrossRef](#)]
24. Lyu, T.; Liu, W.; Hu, Z.; Xiang, X.; Liu, T.; Xiong, X.; Cao, J. Molecular characterization and expression analysis reveal the roles of Cys2/His2 zinc-finger transcription factors during flower development of *Brassica rapa* subsp. *Chinensis*. *Plant Mol. Biol.* **2020**, *102*, 123–141. [[CrossRef](#)]
25. Lu, X.; Li, Y.; Su, Y.; Liang, Q.; Meng, H.; Li, S.; Shen, S.; Fan, Y.; Zhang, C. An *Arabidopsis* gene encoding a C<sub>2</sub>H<sub>2</sub>-domain protein with alternatively spliced transcripts is essential for endosperm development. *J. Exp. Bot.* **2012**, *63*, 5935–5944. [[CrossRef](#)] [[PubMed](#)]

26. Huang, F.; Chi, Y.; Meng, Q.; Gai, J.; Yu, D. *Gmzfp1* encoding a single zinc finger protein is expressed with enhancement in reproductive organs and late seed development in soybean (*Glycine max*). *Mol. Biol. Rep.* **2006**, *33*, 279–285. [[CrossRef](#)] [[PubMed](#)]
27. Mittler, R.; Kim, Y.; Song, L.; Coutu, J.; Coutu, A.; Ciftci-Yilmaz, S.; Lee, H.; Stevenson, B.; Zhu, J.-K. Gain- and loss-of-function mutations in *Zat10* enhance the tolerance of plants to abiotic stress. *FEBS Lett.* **2006**, *580*, 6537–6542. [[CrossRef](#)] [[PubMed](#)]
28. Shi, H.; Liu, G.; Wei, Y.; Chan, Z. The zinc-finger transcription factor ZAT6 is essential for hydrogen peroxide induction of anthocyanin synthesis in *Arabidopsis*. *Plant Mol. Biol.* **2018**, *97*, 165–176. [[CrossRef](#)]
29. Kubo, K.; Kanno, Y.; Nishino, T.; Takatsuji, H. Zinc-Finger genes that specifically express in pistil secretory tissues of petunia. *Plant Cell Physiol.* **2000**, *41*, 377–382. [[CrossRef](#)] [[PubMed](#)]
30. Jenkins, T.H.; Li, J.; Scutt, C.P.; Gilmartin, P.M. Analysis of members of the *Silene latifolia* Cys2/His2 zinc-finger transcription factor family during dioecious flower development and in a novel stamen-defective mutant *ssf1*. *Planta* **2005**, *220*, 559–571. [[CrossRef](#)] [[PubMed](#)]
31. Seibel, N.M.; Eljouni, J.; Nalaskowski, M.M.; Hampe, W. Nuclear localization of enhanced green fluorescent protein homomultimers. *Anal. Biochem.* **2007**, *368*, 95–99. [[CrossRef](#)]
32. Remans, T.; Smeets, K.; Opdenakker, K.; Mathijssen, D.; Vangronsveld, J.; Cuypers, A. Normalisation of real-time RT-PCR gene expression measurements in *Arabidopsis thaliana* exposed to increased metal concentrations. *Planta* **2008**, *227*, 1343–1349. [[CrossRef](#)]
33. Livak, K.J.; Schmittgen, T.D. Analysis of relative gene expression data using real-time quantitative PCR and the  $2^{-\Delta\Delta CT}$  method. *Methods* **2001**, *25*, 402–408. [[CrossRef](#)] [[PubMed](#)]
34. Peterson, R.; Slovin, J.P.; Chen, C. A simplified method for differential staining of aborted and non-aborted pollen grains. *Int. J. Plant Biol.* **2010**, *1*, 66–69. [[CrossRef](#)]
35. Alexander, M.P. Differential staining of aborted and nonaborted pollen. *Stain Technol.* **1969**, *44*, 117–122. [[CrossRef](#)]
36. Impe, D.; Reitz, J.; Köpnick, C.; Rolletschek, H.; Börner, A.; Senula, A.; Nagel, M. Assessment of pollen viability for wheat. *Front. Plant Sci.* **2020**, *10*, 1588. [[CrossRef](#)] [[PubMed](#)]
37. Verma, P.; Majee, M. Seed Germination and Viability Test in Tetrazolium (TZ) Assay. *Bio-Protocol* **2013**, *3*, e884. [[CrossRef](#)]
38. Ciftci-Yilmaz, S.; Mittler, R. The zinc finger network of plants. *Cell. Mol. Life Sci.* **2008**, *65*, 1150–1160. [[CrossRef](#)]
39. Vogel, J.T.; Zarka, D.G.; Van Buskirk, H.A.; Fowler, S.G.; Thomashow, M.F.; Lansing, E. Roles of the CBF2 and ZAT12 transcription factors in configuring the low temperature transcriptome of *Arabidopsis*. *Plant J.* **2005**, 195–211. [[CrossRef](#)] [[PubMed](#)]
40. Rizhsky, L.; Davletova, S.; Liang, H.; Mittler, R. The Zinc Finger Protein Zat12 is required for cytosolic Ascorbate Peroxidase 1 expression during oxidative stress in *Arabidopsis*. *J. Biol. Chem.* **2004**, *279*, 11736–11743. [[CrossRef](#)] [[PubMed](#)]
41. Sakamoto, H.; Araki, T.; Meshi, T.; Iwabuchi, M. Expression of a subset of the *Arabidopsis* Cys2 / His2 -type zinc-finger protein gene family under water stress. *Gene* **2000**, *248*, 23–32. [[CrossRef](#)]
42. Ciftci-Yilmaz, S.; Morsy, M.R.; Song, L.; Coutu, A.; Krizek, B.A.; Lewis, M.W.; Warren, D.; Cushman, J.; Connolly, E.L.; Mittler, R. The EAR-motif of the Cys2/His2-type zinc finger protein Zat7 plays a key role in the defense response of *Arabidopsis* to salinity stress. *J. Biol. Chem.* **2007**, *282*, 9260–9268. [[CrossRef](#)] [[PubMed](#)]
43. Hafidh, S.; Fila, J.; Honys, D. Male gametophyte development and function in angiosperms: A general concept. *Plant Reprod.* **2016**, *29*, 31–51. [[CrossRef](#)] [[PubMed](#)]
44. Steinhorst, L.; Kudla, J. Calcium—A central regulator of pollen germination and tube growth. *Biochim. Biophys. Acta* **2012**, *1833*, 1573–1581. [[CrossRef](#)]
45. Johnson, M.A.; Harper, J.F.; Palanivelu, R. A fruitful journey: Pollen tube navigation from germination to fertilization. *Annu. Rev. Plant Biol.* **2019**, *70*, 809–837. [[CrossRef](#)]
46. Vivian-Smith, A.; Luo, M.; Chaudhury, A.; Koltunow, A. Fruit development is actively restricted in the absence of fertilization in *Arabidopsis*. *Development* **2001**, *128*, 2321–2331. [[CrossRef](#)]
47. Nguyen Ba, A.N.; Pogoutse, A.; Provart, N.; Moses, A.M. NLStradamus: A simple Hidden Markov Model for nuclear localization signal prediction. *BMC Bioinform.* **2009**, *10*, 202. [[CrossRef](#)]
48. Kumar, S.; Stecher, G.; Li, M.; Nnyaz, C.; Tamura, K. MEGA X: Molecular evolutionary genetics analysis across computing platforms. *Mol. Biol. Evol.* **2018**, *35*, 1547–1549. [[CrossRef](#)]
49. Thompson, J.D.; Higgins, D.G.; Gibson, T.J. CLUSTAL W: Improving the sensitivity of progressive multiple sequence alignment through sequence weighting, position-specific gap penalties and weight matrix choice. *Nucleic Acids Res.* **1994**, *22*, 4673–4680. [[CrossRef](#)]
50. Hall, T. Bioedit: An important software for molecular biology. *GERF Bull. Biosci.* **2011**, *2*, 60–61.
51. Blum, M.; Chang, H.; Chuguransky, S.; Grego, T.; Kandasaamy, S.; Mitchell, A.; Nuka, G.; Paysan-lafosse, T.; Qureshi, M.; Raj, S.; et al. The interpro protein families and domains database: 20 years on. *Nucleic Acids Res.* **2021**, *49*, 344–354. [[CrossRef](#)] [[PubMed](#)]
52. Ohta, M.; Matsui, K.; Hiratsu, K.; Shinshi, H.; Ohme-Takagi, M. Repression Domains of Class II ERF Transcriptional Repressors Share an Essential Motif for Active Repression. *Plant Cell* **2001**, *13*, 1959–1968. [[CrossRef](#)]
53. Saitou, N.; Nei, M. The Neighbor-joining method: A new method for reconstructing phylogenetic trees. *Mol. Biol. Evol.* **1987**, *4*, 406–425. [[CrossRef](#)]
54. Felsenstein, J. Confidence limits on phylogenies: An approach using the bootstrap. *Evolution* **1985**, *39*, 783–791. [[CrossRef](#)] [[PubMed](#)]

55. Cardarelli, M.; Cecchetti, V. Auxin polar transport in stamen formation and development: How many actors? *Front. Plant Sci.* **2014**, *5*, 333. [[CrossRef](#)] [[PubMed](#)]
56. Smyth, D.R.; Bowman, J.L.; Meyerowitz, E.M. Early flower development in *Arabidopsis*. *Plant Cell* **1990**, *2*, 755–767. [[CrossRef](#)]
57. Porter, R.; Durrel, M.; Romm, H.J. The use of 2,3,5-triphenyl-tetrazolium chloride as a measure of seed germinability. *Plant Physiol.* **1946**, *22*, 149–159. [[CrossRef](#)]
58. Verma, P.; Kaur, H.; Petla, B.P.; Rao, V.; Saxena, S.C.; Majee, M. *PROTEIN L-ISOASPARTYL METHYLTRANSFERASE2* is by reducing abnormal isoaspartyl accumulation predominantly in seed nuclear proteins. *Plant Physiol.* **2013**, *161*, 1141–1157. [[CrossRef](#)]